pean Space Technology Center and the Jet Propulsion Laboratory and the spacecraft and mission operations teams of the European Space Association and the National Aeronautics and Space Administration for help and cooperation in carrying out this experiment. We thank M. Bruns and S. Mazuk for their work in preparing the data, G. Umlauft and K. Fischer for their work in building and calibrating the instrument, W. I. Axford and V. M. Vasyliunas for discussions and suggestions, and A. Balogh and B. Forsythe for supplying data in advance of publication. This work was supported by the Max Planck Gesellschaft, by the Deutsche Agentur für Raumfahrtangelegenheiten under grant number 50ON91050 (MPAE part). Work at Imperial College was supported by the United Kingdom Science and Engineering Research Council and at Kiruna by the Swedish National Space Board.

27 May 1992; accepted 31 July 1992

Regulation of Dynein-Driven Microtubule Sliding by the Radial Spokes in Flagella

Elizabeth F. Smith and Winfield S. Sale

The regulation of microtubule sliding in flagellar axonemes was studied with the use of *Chlamydomonas* mutants and in vitro assays. Microtubule sliding velocities were diminished in axonemes from mutant cells missing radial spoke structures but could be restored upon reconstitution with dynein from axonemes with wild-type radial spokes. These experiments demonstrate that the radial spokes activate dynein's microtubule sliding activity.

Dyneins are a family of adenosine triphosphatases that cause microtubule sliding in ciliary and flagellar axonemes (*1–3*) and directed vesicle transport along cytoplasmic microtubules (*4*). Although much is known about the structure and action of axonemal dyneins (*5*), little is known about how their activity is regulated or how active microtubule sliding is translated into principal and reverse bends. Because dynein generates force in a single direction relative to microtubule polarity (*6*), and because variation in microtubule sliding along the length of the axoneme appears to generate bends (*3, 7*), dynein-driven microtubule sliding must be regulated spatially and temporally.

Structural (*8*) and genetic (*9*) evidence implicates the radial spokes as regulatory components. The spokes are protein complexes (*10, 11*) that attach to each doublet microtubule immediately adjacent to the inner row of dynein arms and project centrally (Figs. 1 and 2A). Mutants of the biflagellate alga *Chlamydomonas* that are deficient in radial spokes either are paralyzed or have altered motility (*9, 11*). Certain suppressor mutations that bypass the requirement of normal radial spokes for motility contain defects in the dynein arms (*12, 13*). To test the hypothesis that radial spokes interact with dynein, we analyzed microtubule sliding velocities in isolated axonemes from mutant strains of *Chlamydomonas*.

In the sliding disintegration assay (*14*), flagellar axonemes are isolated, treated with protease, and exposed to adenosine triphosphate (ATP) that induces the doublet microtubules to slide apart in a telescoping fashion (*15–17*). Thus, dynein-induced doublet microtubule sliding velocities can be uncoupled from flagellar bending and quantified in both paralyzed and motile mutants (*18, 19*). Altered sliding velocities would reflect an interaction between spokes and dynein. We found that the spokeless mutant (*pf*14, which had paralyzed flagella) had sliding velocities (2.0 ± 0.9 μm/s, $n = 51$) that were significantly slower ($P < 0.001$) than those of wild type (6.1 ± 1.4 μm/s, $n = 34$) (*15*). Therefore, in the absence of the radial spokes dynein (either inner or outer arms) is apparently not as efficient in translocating the doublet microtubules.

We focused our study on the inner dynein arms because they are necessary and sufficient for motility (*18*) and have features that suggest they might be targets of regulation (*13, 19–21*). The three subtypes of inner dynein arms are located in distinct positions in the axoneme, perhaps indicating functional specialization (*20*). Several inner arm components are phosphoproteins (*21*), and defects in phosphorylation may suppress paralysis in mutants without radial spokes (*13*). The spokes are also located immediately adjacent to the inner dynein arms, perhaps providing direct structural interactions. Finally, the inner dynein arms can be structurally and functionally reconstituted in vitro (*19*), which provides a new experimental approach for the exchange of dynein arms on axonemes of distinct composition.

We compared the sliding velocities of a mutant without outer dynein arms, *pf*28 (motile flagella), with those of a mutant that lacks both radial spokes and outer dynein arms, *pf*14*pf*28 (immotile flagella) (Fig. 2). Axonemes from *pf*14*pf*28 had significantly ($P < 0.001$) slower sliding velocities (*15*) (0.5 ± 0.2 μm/s, $n = 42$) than *pf*28 axonemes (1.3 ± 0.5 μm/s, $n = 43$), indicating that the presence or absence of spokes affects the microtubule-translocating efficiency of the inner dynein arms. To determine whether dynein was activated through a modification induced by the spokes, we used an in vitro reconstitution system (*19*) to switch the inner dynein arms of *pf*28 axonemes with those of *pf*14*pf*28 axonemes.

Reconstitution experiments with inner dynein arms that had (in *pf*28) or had not (in *pf*14*pf*28) been exposed to spokes indicated that the radial spokes induced a modification of the inner dynein arms that was maintained in the subsequent absence of radial spokes (Table 1). Both *pf*28 and *pf*14*pf*28 axonemes reconstituted with their respective extracts slid at their original velocities, indicating that the extraction and reconstitution procedure did not by itself induce any changes in dynein activity. Extracted axonemes from *pf*28 reconstituted with inner arms from *pf*14*pf*28 slid at the velocity of intact *pf*28 axonemes. Furthermore, extracted axonemes from *pf*14*pf*28 reconstituted with inner arms from *pf*28 also slid at the velocity of intact *pf*28 axonemes. Therefore, the inner dynein arms from *pf*28 exposed to radial spokes remain in an activated state after extraction and reconstitution without the radial spokes.

Similar results were obtained in a potassium acetate (KCH_3COO) buffer (Table 1), which was reported to produce microtubule sliding velocities that closely parallel those calculated for beating, reactivated axonemes (*22*). Although all sliding velocities increased, their relative differences were not affected.

The increased sliding velocity of *pf*14*pf*28 axonemes reconstituted with inner

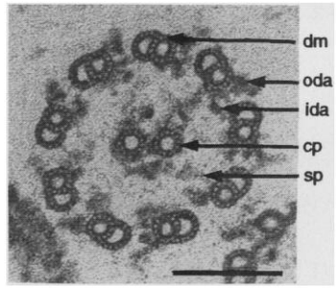

Fig. 1. Electron micrograph of axonemal cross section from wild-type *Chlamydomonas* flagella indicating the doublet microtubules (dm), outer (oda) and inner (ida) dynein arms, central pair of microtubules (cp), and radial spokes (sp). Axonemes were isolated and prepared for electron microscopy as described in (*19*). Scale bar, 100 nm.

Department of Anatomy and Cell Biology, Emory University School of Medicine, Atlanta, GA 30322.

Table 1. Microtubule sliding velocities (in micrometers per second) of axonemes induced by 1 mM ATP; ex, dynein-containing high-salt extract; exax, high-salt extracted axonemes.

Cell type of axoneme source	NaCl buffer (*n*)	KCH_3COO buffer (*n*)	Reconstituted with inner arms from *pf*28 ex (*n*)		Reconstituted with inner arms from *pf*14*pf*28 ex (*n*)	
			NaCl buffer	KCH_3COO buffer	NaCl buffer	KCH_3COO buffer
*pf*28	1.3 ± 0.5 (43)	2.7 ± 0.5 (22)				
*pf*14*pf*28	0.5 ± 0.2 (42)	1.0 ± 0.3 (23)				
*pf*28 exax			1.3 ± 0.5 (41)	2.6 ± 0.9 (21)	1.3 ± 0.5 (18)	2.8 ± 1.0 (22)
*pf*14*pf*28 exax			1.2 ± 0.3 (20)	2.6 ± 0.7 (28)	0.5 ± 0.2 (15)	0.8 ± 0.3 (10)

arms from *pf*28 was not due to dynein arms binding to extraneous positions on the extracted *pf*14*pf*28 axonemes. Although this possibility seemed unlikely (*19*), we examined the reconstituted axonemes by electron microscopy. The inner dynein arms reattached solely to inner arm positions and did not bind to any inappropriate positions even at supersaturating ratios of dynein to axonemes. Addition of excess amounts of inner dynein arms did not result in increased sliding velocities in the sliding disintegration assay (Fig. 3). At ratios of dynein to axonemes of 2:1, 4:1, and 10:1 no significant differences were found in sliding velocity, and in no case did mean sliding velocities exceed that of *pf*28 axonemes (Fig. 3).

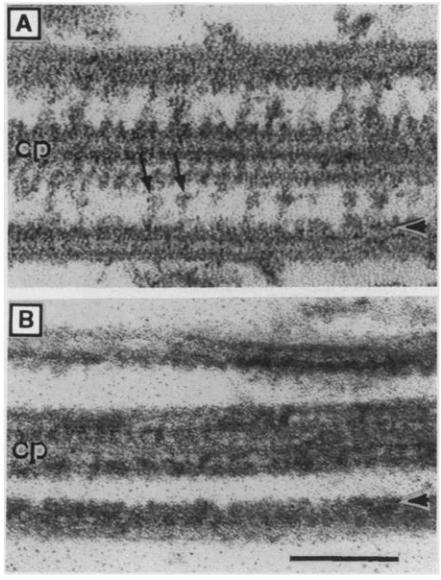

Fig. 2. Electron micrographs of longitudinal sections through (**A**) *pf*28 and (**B**) *pf*14*pf*28 axonemes. The inner arm organization (arrowheads) of *pf*14*pf*28 does not differ from that of *pf*28 (*10, 20, 23*). Arrows indicate radial spokes. Cp, central pair of microtubules. Bar, 100 nm.

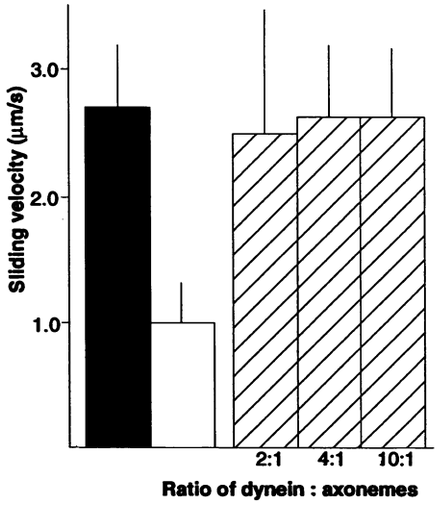

Fig. 3. Microtubule sliding velocities for *pf*28 (shaded), *pf*14*pf*28 (white), and *pf*14*pf*28 (hatched) extracted axonemes reconstituted with dynein from *pf*28 axonemes. Reconstitution and sliding disintegration were performed as described (*15*). The ratios of dynein to extracted axonemes are based on fixed volume ratios at initial protein concentrations of axonemes of 0.5 mg/ml (*19*). Vertical lines above bars, SEM.

The increased sliding velocity of the reconstituted *pf*14*pf*28 axonemes was not due to transfer of the "activating factor" (spoke components and enzymes) in extracts from the *pf*28 axonemes onto the *pf*14*pf*28 axonemes. In both sodium chloride (NaCl) and KCH_3COO buffers, the doublet microtubules of *pf*28 extracted axonemes reconstituted with *pf*14*pf*28 inner dynein arms had rapid sliding velocities (Table 1), indicating that the dynein activator remained associated with extracted *pf*28 axonemes. This experiment also revealed that the *pf*14*pf*28 inner arm dyneins can induce the more rapid sliding velocities characteristic of *pf*28 axonemes when these dyneins have been exposed to the radial spokes. Therefore, there is no inherent defect in the inner arms of *pf*14*pf*28 that would account for the original slow microtubule sliding velocities.

Differences in microtubule sliding velocities were not a consequence of differences in inner arm composition associated with flagella of varying length (*20*). Short flagella such as those in *pf*14*pf*28 are missing inner arm heavy chain 3′ and contain a reduced amount of heavy chain 2, compared with those in *pf*28 (*20*). To test the possibility that this difference in composition resulted in slow microtubule sliding velocities, we assayed sliding disintegration with a paralyzed mutant (*pf*13A) that lacks outer dynein arms, contains radial spokes, has the identical inner arm heavy chain composition as *pf*14*pf*28, and has short flagella. In the NaCl buffer the *pf*13A axonemes slid at slightly faster velocities than *pf*28 axonemes, and in the KCH_3COO buffer velocities of *pf*13 and *pf*28 were almost the same (Table 2). Therefore, the

Table 2. Microtubule sliding velocity of nagarse-treated mutant axonemes induced by 1 mM ATP.

Cell type	Missing structure	Velocity μm/s (*n*) NaCl buffer	Velocity μm/s (*n*) K acetate buffer
	Strains with normal spokes		
137*c*	None	6.1 ± 1.4 (34)	12.1 ± 2.9 (19)
*pf*28	Outer dynein arms	1.3 ± 0.5 (43)	2.7 ± 0.5 (22)
*pf*13A (*20*)	Outer dynein arms, inner arm heavy chain 3′	1.9 ± 0.8 (17)	2.8 ± 1.2 (17)
*sup-pf*1 (*12*)	Suppressor	6.4 ± 1.6 (20)	13.0 ± 3.4 (21)
	Strains with defective spokes		
*pf*14 (*11*)	Spokes	2.0 ± 0.9 (51)	5.6 ± 1.4 (18)
*pf*14*pf*28 (*20*)	Spokes, outer arms	0.5 ± 0.2 (42)	1.0 ± 0.3 (23)
*pf*1 (*11*)	Spokeheads	2.9 ± 1.4 (27)	4.8 ± 1.6 (28)
*pf*17 (*10*)	Spokeheads	2.4 ± 0.9 (20)	4.3 ± 1.7 (22)
*pf*27 (*10*)	Unphosphorylated*	1.2 ± 0.5 (23)	4.5 ± 1.4 (25)
*sup-pf*1*pf*17 (*12*)	Spokeheads, suppressor mutation	4.9 ± 1.5 (23)	6.5 ± 2.0 (23)

*Certain radial spoke proteins that are normally phosphorylated are not phosphorylated in this mutant (*10*).

slow microtubule sliding velocities in *pf*14*pf*28 are not due to the lack of inner arm heavy chain 3′.

We tested whether inner arm heavy chain 3′ was the activating factor by reconstituting *pf*14*pf*28 axonemes with inner arms from *pf*13A. The resulting sliding velocities were not significantly different from those obtained with extracts from *pf*28 axonemes (1.5 ± 0.3 μm/s, n = 14 in NaCl; 2.4 ± 0.7 μm/s, n = 29 in KCH_3COO). Because the only difference between *pf*13A and *pf*14*pf*28 is the presence or absence of spokes, our results with extracts from *pf*28 cannot be explained by the contribution of a subset of inner arms from *pf*28 axonemes.

Our interpretation is that the spokes activate the inner dynein arms by a modification that survives high salt extraction and dialysis required for reconstitution. [Certain inner arm subforms may be differentially affected (*20*).] This interpretation was supported by comparison of sliding velocities of other axonemes defective for radial spokes (those of *pf*14, *pf*1, *pf*17, and *pf*27) with wild-type axonemes (those of 137c). Axonemal microtubules from all of these mutants slid at one-half to one-third the velocity of wild-type microtubules in both buffer conditions (Table 2), indicating that reduced microtubule sliding velocities are not unique to the *pf*14 mutation and that the outer arms cannot overcome the inactivation caused by the lack of radial spokes. Outer dynein arm activity might also be affected by the spokes in wild-type axonemes, as suggested by an unusual class of suppressor mutants (*sup-pf*1) in which the requirement of radial spokes for movement is bypassed by a defect in the beta heavy chain of the outer dynein arms (*12*). Calculations of sliding velocities (*12*) and those measured from sliding disintegration (those of *pf*17, compared with those of *sup-pf*1*pf*17 and *sup-pf*1, Table 2) indicate that the suppressor mutation increases microtubule sliding velocities in the absence of the spokes. Our results indicate activation of dynein-induced microtubule sliding activity by the radial spokes.

REFERENCES AND NOTES

1. P. Satir, *J. Cell Biol.* **39**, 77 (1968).
2. K. E. Summers and I. R. Gibbons, *Proc. Natl. Acad. Sci. U.S.A.* **68**, 3092 (1971).
3. C. J. Brokaw, *Science* **243**, 1593 (1989).
4. G. S. Bloom, *Curr. Opin. Cell Biol.* **4**, 66 (1992).
5. G. B. Witman, *ibid.*, p. 77; K. A. Johnson, *Annu. Rev. Biophys. Biophys. Chem.* **14**, 161 (1985).
6. W. S. Sale and P. Satir, *Proc. Natl. Acad. Sci. U.S.A.* **74**, 2045 (1977); L. A. Fox and W. S. Sale, *J. Cell Biol.* **105**, 1781 (1987).
7. C. J. Brokaw, *J. Cell Biol.* **114**, 1201 (1991).
8. F. D. Warner and P. Satir, *ibid.* **63**, 35 (1974); C. Omoto and C. Kung, *ibid.* **87**, 33 (1980).
9. B. Huang, *Int. Rev. Cytol.* **99**, 181 (1986).
10. G. Piperno, B. Huang, Z. Ramanis, D. J. L. Luck, *J. Cell Biol.* **88**, 73 (1981); B. Huang, G. Piperno, Z. Ramanis, D. J. L. Luck, *ibid.*, p. 80.
11. D. Luck, G. Piperno, Z. Ramanis, B. Huang, *Proc. Natl. Acad. Sci. U.S.A.* **74**, 3456 (1977); D. R. Diener *et al.*, *ibid.* **87**, 5739 (1990).
12. B. Huang, Z. Ramanis, D. J. L. Luck, *Cell* **28**, 115 (1982); C. J. Brokaw, B. Huang, D. J. L. Luck, *J. Cell Biol.* **92**, 722 (1982); C. J. Brokaw and R. Kamiya, *Cell Motil. Cytoskeleton* **8**, 68 (1987).
13. D. J. L. Luck and G. Piperno, in *Cell Movement: The Dynein ATPases*, F. D. Warner, P. Satir, I. R. Gibbons, Eds. (Liss, New York, 1989), vol. 1, chap. 4.
14. G. B. Witman, J. Plummer, G. Sander, *J. Cell Biol.* **76**, 729 (1978).
15. Flagella were isolated by the dibucaine method and resuspended in a buffer containing 10 mM Hepes (pH 7.4), 5 mM $MgSO_4$, 1 mM dithiothreitol (DTT), 0.5 mM EDTA, and 30 mM NaCl (NaCl buffer) with 0.1 mM phenylmethylsulfonyl fluoride and 0.6 trypsin inhibitor unit aprotinin, 4°C, and remained in this buffer until sliding disintegration was performed with the methods of Okagaki and Kamiya (*16*), with modifications as described in (*19*). As Tables 1 and 2 indicate, sliding disintegration was also performed in a KCH_3COO buffer [30 mM Hepes (pH 7.4), 5 mM $MgSO_4$, 1 mM DTT, 1.0 mM EGTA, 50 mM KCH_3COO, and 0.5% polyethylene glycol] (*22*). Axonemes were prepared as above except that adherent axonemes were washed with KCH_3COO buffer and sliding was induced by perfusion with the KCH_3COO buffer containing 1 mM ATP and nagarose (1 to 2 μg/ml). All sliding disintegration was recorded on videotape with a silicone intensified target camera and dark-field microscopy as described in (*16*). Analysis was restricted to axonemes in which sliding between pairs of microtubules or pairs of microtubule groups could be distinguished. Performing sliding disintegration with extracted axonemes in reconstitution experiments did not require prior sonication. Sliding velocities were measured manually from the video screen.
16. T. Okagaki and R. Kamiya, *J. Cell Biol.* **103**, 1895 (1986).
17. C. J. Brokaw, *Science* **207**, 1365 (1980).
18. R. Kamiya, E. Kurimoto, H. Sakakibara, T. Okagaki, in (*13*), chap. 15.
19. E. F. Smith and W. S. Sale, *J. Cell Biol.* **117**, 573 (1992).
20. G. Piperno, Z. Ramanis, E. F. Smith, W. S. Sale, *ibid.* **110**, 379 (1990); G. Piperno and Z. Ramanis, *ibid.* **112**, 701 (1991).
21. G. Piperno and D. J. L. Luck, *Cell* **27**, 331 (1981).
22. E. Kurimoto and R. Kamiya, *Cell Motil. Cytoskeleton* **19**, 275 (1991).
23. E. Muto, R. Kamiya, S. Tsukita, *J. Cell Sci.* **99**, 57 (1991).

24. We thank G. Piperno for helpful discussion and for mutant strains of *Chlamydomonas*. Supported by NIH research grant HD 20497 and training grant GM 08367.

30 April 1992; accepted 9 July 1992

NMR Determination of Residual Structure in a Urea-Denatured Protein, the 434-Repressor

Dario Neri,* Martin Billeter, Gerhard Wider, Kurt Wüthrich†

A nuclear magnetic resonance (NMR) structure determination is reported for the polypeptide chain of a globular protein in strongly denaturing solution. Nuclear Overhauser effect (NOE) measurements with a 7 molar urea solution of the amino-terminal 63-residue domain of the 434-repressor and distance geometry calculations showed that the polypeptide segment 54 to 59 forms a hydrophobic cluster containing the side chains of Val^{54}, Val^{56}, Trp^{58}, and Leu^{59}. This residual structure in the urea-unfolded protein is related to the corresponding region of the native, folded protein by simple rearrangements of the residues 58 to 60. Based on these observations a model for the early phase of refolding of the 434-repressor(1-63) is proposed.

Investigations of proteins in strongly denaturing solution are of general interest relative to the protein folding problem (*1*, *2*). For example, strongly denaturing solutions are often used as the "random-coil" reference state in refolding studies, and residual nonrandom structure found under such conditions might be indicative of nucleation sites for the refolding process. Structure determinations of partially or fully unfolded polypeptides are intrinsically difficult, and structural data on such species are scarce. Here we use the NMR method that is now in widespread use for studies of native, folded proteins (*3*, *4*) for a structure determination of the urea-unfolded form of the amino-terminal 63-residue domain of the 434-repressor.

For a polypeptide consisting of the amino-terminal residues 1 to 69 of the 434-repressor, which includes the DNA-binding domain (*5*), the three-dimensional structure has been determined at high resolution by x-ray diffraction in single crystals (*6*) and by NMR in solution (*7*). The same molecular architecture with five α helices was observed in the crystals and in solution, and in both states the carboxyl-terminal peptide of residues 64 to 69 was found to be unstructured. Initial studies of urea denaturation showed that the native, folded form and an unfolded form coexist over a wide range of urea concentrations at pH 4.8 and 18°C (*8*). In the absence of urea, only the NMR spectrum of the folded protein is seen. In 4.2 M urea, the two forms are present in equal concentrations and have an exchange life time of ~1 s. In 7 M urea,

Institut für Molekularbiologie und Biophysik, ETH-Hönggerberg, CH-8093 Zürich, Switzerland.

*Present address: Cambridge Centre for Protein Engineering, Hills Road, Cambridge CB2 2QII, United Kingdom.

†To whom correspondence should be addressed.